Neural Comput & Applic (2014) 25:879–888
DOI 10.1007/s00521-014-1561-9

ORIGINAL ARTICLE

# Fuzzy logic controller and cascade inverter for direct torque control of IM

**Rasoul Rahmani · Nima M. A. Langeroudi · Rozbeh Yousefi · Milad Mahdian · Mohammadmehdi Seyedmahmoudian**

Received: 9 December 2013 / Accepted: 4 March 2014 / Published online: 2 April 2014


**Abstract** In this paper, a five-level cascaded H-bridge multilevel inverters topology is applied on induction motor control known as direct torque control (DTC) strategy. More inverter states can be generated by a five-level inverter which improves voltage selection capability. This paper also introduces two different control methods to select the appropriate output voltage vector for reducing the torque and flux error to zero. The first is based on the conventional DTC scheme using a pair of hysteresis comparators and look up table to select the output voltage vector for controlling the torque and flux. The second is based on a new fuzzy logic controller using Sugeno as the inference method to select the output voltage vector by replacing the hysteresis comparators and lookup table in the conventional DTC, to which the results show more reduction in torque ripple and feasibility of smooth stator current. By using Matlab/Simulink, it is verified that using five-level inverter in DTC drive can reduce the torque ripple in comparison with conventional DTC, and further torque ripple reduction is obtained by applying fuzzy logic controller. The simulation results have also verified that using a fuzzy controller instead of a hysteresis controller has resulted in reduction in the flux ripples significantly as well as reduces the total harmonic distortion of the stator current to below 4 %.

**Keywords** DTC · Five-level cascaded H-bridge inverter · Fuzzy logic controller · Induction motor

R. Rahmani (✉) · R. Yousefi
Centre for Artificial Intelligence and Robotics, Universiti Teknologi Malaysia, Jalan Semarak, 54100 Kuala Lumpur, Malaysia
e-mail: rahmani@ic.utm.my

N. M. A. Langeroudi
Faculty of Built Environment, Heriot-Watt University, Edinburgh, UK

M. Mahdian
Mechatronics Group, Islamic Azad University, Khomeinishahr Branch, Esfahān, Iran

M. Seyedmahmoudian
School of Engineering, Deakin University, Geelong, Australia

## 1 Introduction

In recent decades, induction motors have received considerable amount of attention among engineers in medium- and high-power industrial applications. The main advantages of induction motors over DC motors are their low cost and maintenance, reliability and high efficiency. On the other hand, induction motors are considerably multivariable, complex and highly coupled systems which make their precise control process computationally expensive and ineffective in many cases. Recent advances in power electronics and computing have made the use of induction motors efficient and feasible in terms of computational cost and performance.

Direct torque control (DTC) was first proposed by Takahashi in 1986, as a control strategy for induction motors. The Basic idea behind such a high-performance induction motor drive is decouple control of torque and also stator flux which yields fast torque response and high-efficiency operation [1, 2]. In DTC strategy, the control of torque and speed is directly based on the electromagnetic state of the motor [3]. The major advantages of DTC can be listed as having a simple structure (no need for complicated coordinate transformation, current regulation or modulation block), fast torque response, and robustness against motor

parameter variation [4–6]. In contrast, it comes with disadvantages such as requiring flux and torque estimator, and also generating ripples in torque and flux [7]. Torque ripple is a major problem of AC motor drives. In high-power applications, the inverter's switching work in low power mode to reduce the power loss which is achieved by applying widening the flux and torque hysteresis band. The wider the hysteresis band is applied, the larger the torque ripple emerges, which sometimes reaches an undesired level. There are various implementation methods which are proposed to solve this problem that in a way increase the complexity of the DTC drive. These include the use of predictive control scheme [8, 9], space vector modulation (SVM) technique [10–13] and artificial intelligence (AI)-based techniques [14–18]. Fuzzy logic is used in different control strategies of induction machines which has shown better control quality compared with the conventional methods [19–21].

Multilevel inverter is another strategy which plays an important role in reducing torque and flux ripples, which provides more practical solutions for engineers in induction motor applications. A wide range of multilevel inverter such as diode clamp, fly capacitor and cascaded types have been used in adjustable speed drives. It is well known that by using multilevel inverter topology, the number of inverter states increase, which results in having more inverter switching voltage space vectors to regulate instantaneously the electromagnetic torque and stator flux magnitudes in DTC strategy. Multilevel inverter also generates low d$v$/d$t$ leading to low electromagnetic interference (EMI) and winding insulation stress, which is desirable for high-power and voltage applications [6, 22–25].

Three-level neutral-point-clamped (NPC) inverter is the most common topology in high-power AC drives; however, it does not fulfill all the requirements whenever it is desired that power is provided from more than one source such as series of batteries, fuel cell and ultra-capacitor. Electric vehicle application is one of such applications in which NPS does not perform satisfactor. To overcome this problem, cascaded H-bridge inverter (CHB) is proposed to be used widely in such application. CHB utilizes small inverter bridges with relatively low voltage to synthesize and reach high voltage; thus, it is more suitable for induction motor in EV or HEV. Our previous work was about three-level cascaded multilevel inverter application in induction motor which was shown merits of CHB-MLI as an inverter for controlling motor [26].

The objectives of this paper are reduction in torque ripple and achieving smooth stator current in DTC method by using five-level CHB inverter-based DTC. Two different control methods are introduced to control the torque and flux in DTC. The first is based on the conventional DTC method using a pair of hysteresis comparator and lookup table, and the second is based on a fuzzy DTC method using Sugeno as the inference method to select the output voltage vector for minimizing the torque and flux error to zero.

## 2 Basic concepts of DTC

The basic concept of DTC is instant regulation of torque and stator flux magnitude by using proper selection of space vector voltage resulted by six-step inverter. The major parts of DTC drive are a pair of hysteresis comparator, flux and torque estimators, voltage vector selector and a voltage source inverter (VSI) [2]. Hysteresis controllers generate two or three levels of signal which present flux or torque error status, respectively. The main feature of hysteresis controller is having no difference between large and small error of torque. When the error value passes from a bandwidth, hysteresis controller will generate the appropriate signal which can be 1, 0 or −1. Depending on the error status of torque and flux, VSI can generate proper voltage to apply stator for keeping stator flux in specific bandwidth. The major advantage of DTC is using separate control of the stator flux and torque, which is also known as decouple control. By use of space vector in a stationary frame, an induction motor can be modeled mathematically, which can be expressed as:

$$v_{\mathrm{s}} = R_{\mathrm{s}} i_{\mathrm{s}} + \frac{\mathrm{d}\phi_{\mathrm{s}}}{\mathrm{d}t} \tag{1}$$

$$0 = R_{\mathrm{r}} i_{\mathrm{r}} + \frac{\mathrm{d}\phi_{\mathrm{r}}}{\mathrm{d}t} - j\omega_{\mathrm{r}}\phi_{\mathrm{r}} \tag{2}$$

$$\phi_{\mathrm{s}} = L_{\mathrm{s}} i_{\mathrm{s}} + L_{\mathrm{m}} i_{\mathrm{r}} \tag{3}$$

$$\phi_{\mathrm{r}} = L_{\mathrm{m}} i_{\mathrm{s}} + L_{\mathrm{r}} i_{\mathrm{r}} \tag{4}$$

where $R_{\mathrm{s}}, R_{\mathrm{r}}, L_{\mathrm{s}}, L_{\mathrm{r}}$ and $L_{\mathrm{m}}$ are the stator resistance, rotor resistance, stator inductance; $v_{\mathrm{s}}, i_{\mathrm{r}}, i_{\mathrm{s}}, \phi_{\mathrm{s}}$ and $\phi_{\mathrm{r}}$ are the stator voltage vector, stator current vector, rotor current vector, stator flux linkage vector and rotor flux linkage vector, respectively; and $\omega_{\mathrm{r}}$ is rotor speed. The electromagnetic torque can be expressed in terms of air gap power or voltage and current of stator or rotor.

$$T_{\mathrm{e}} = \frac{3}{2}\frac{P}{2} L_{\mathrm{m}} (i_{\mathrm{qs}}\phi_{\mathrm{ds}} - i_{\mathrm{ds}}\phi_{\mathrm{qs}}) \tag{5}$$

where $T_{\mathrm{e}}, P, \phi_{\mathrm{dr}}$ and $\phi_{\mathrm{ds}}$ are the electromagnetic torque, number of poles, rotor $d-q$ axes fluxes, respectively. The torque developed in an induction motor (Eq. 5) can be expressed in many ways. One such expression in stationary frame reference is:

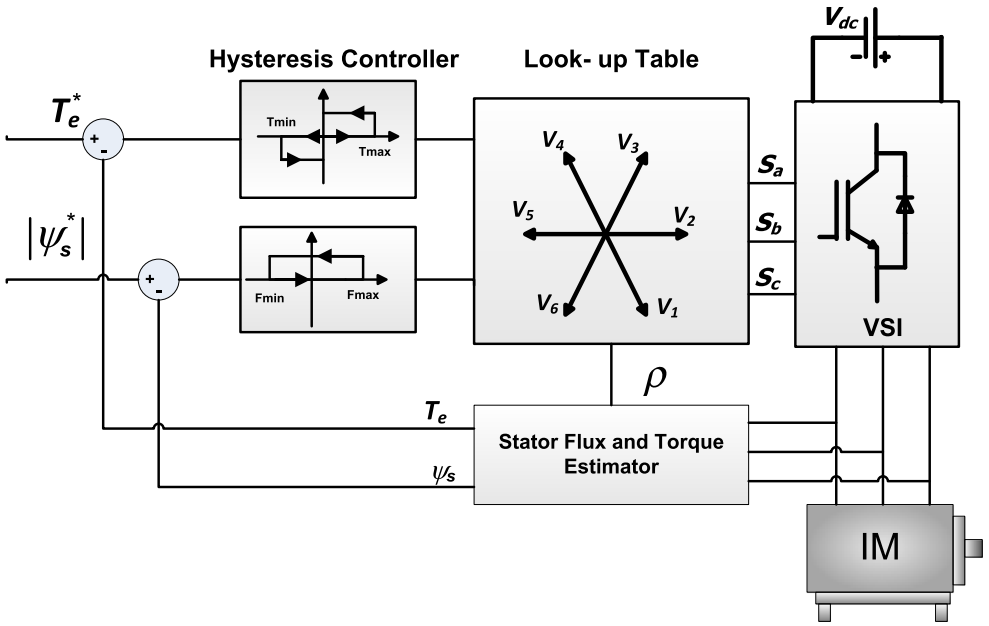


**Fig. 1** Two-level conventional DTC structure

$$T_e = \frac{3}{4}\frac{PL_m}{L_r L_s'}|\phi_r||\phi_s|\sin\gamma \tag{6}$$

where $\gamma$ is the angle between the stator and rotor flux linkage space vectors and $L_s' = L_s L_r - L_m{}^2$. Thus, the torque can be controlled by adjusting $\gamma$. On the other hand, the magnitude of the stator flux can be determined by the stator voltage according to Eq. (7).

$$\phi_s = \int_0^{t_0} (v_s - R_s I_s)\mathrm{d}t \tag{7}$$

Since the rotor time constant of a squirrel-cage IM is very large, the reaction of the rotor flux vector with regard to the stator voltage is somewhat sluggish in comparison with that of the stator flux vector. Also, it should be considered that leakage inductances have low-pass filtering behavior which causes the rotor flux waveform to be smoother than the stator flux. If the stator resistance is small enough to be neglected, the change in stator flux, $\Delta\psi_s$, will follow the stator voltage for a switch-on time $T_s$ of the voltage vector $V_s(\Delta\overline{\psi} = \overline{V_s} \times \Delta t)$. Hence, as can be seen in Eq. (6), $|\phi_s|$ and $\gamma$ are two parameters which are used for controlling electrical torque. According to Takahashi and Noguchi [2], stator flux plane can be divided into six sectors where each sector will have a radial component and a tangential component with respect to the stator flux linkage vector. Figure 1 shows a two-level inverter-based conventional DTC scheme where the proper voltage vector is selected according to the sector and error states of torque and flux.

## 3 Five-level CHB-MLI topology

CHB-MLI is based on a series connection of single-phase VSI bridges, and the earliest reference to them appeared in 1975 [27–29]. Figure 2 indicates the structure of a three-phase cascaded-type inverter. It shows an example of five-level cascaded inverter composed of two full-bridge inverters connected in series on each phase. Each full-bridge converter can produce three levels as $+V_{dc}$, 0, $-V_{dc}$ by using the DC source to the AC output by different combinations of four switches. Following equations show corresponding switching status for one phase, in which each leg in cascade inverter can generate a phase voltage with five voltage levels.

$$v_{out1} = \begin{cases} +V_{dc} & S_{11} \text{ and } S_{12} \text{ On} \\ 0 & S_{11} \text{ and } S_{13} \text{ On} \\ -V_{dc} & S_{13} \text{ and } S_{14} \text{ On} \end{cases} \tag{8}$$

$$v_{out2} = \begin{cases} +V_{dc} & S_{21} \text{ and } S_{22} \text{ On} \\ 0 & S_{21} \text{ and } S_{23} \text{ On} \\ -V_{dc} & S_{23} \text{ and } S_{24} \text{ On} \end{cases} \tag{9}$$

The resultant inverter phase voltage is $V_c = v_{out1} + v_{out2}$, which is the voltage terminal at legIII of inverter with respect to the inverter neutral N. The output voltage can be 0, $V_{dc}$, $2V_{dc}$. There are three legs and five switching status for each phase, so 243 switching status can be generated in which redundancy is inevitable [12]. Some voltage level can be obtained by more than one switching status; it has 61 effective voltage vectors that can be located with specific angle and magnitude in space vector diagram. Figure 3 shows space vector diagram of effective voltages.

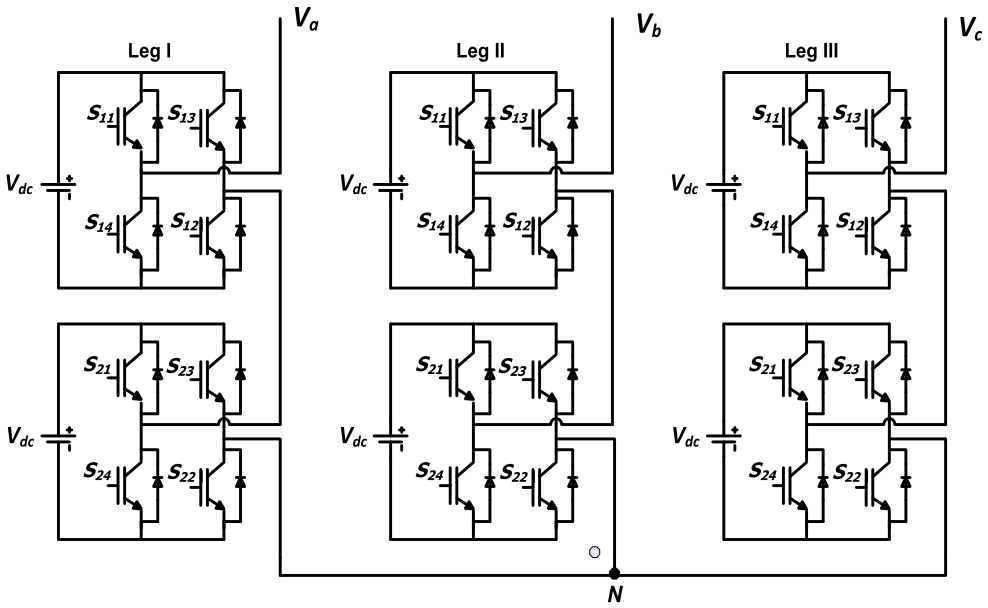


**Fig. 2** Three-phase five-level topology of cascaded H-bridge multilevel inverter

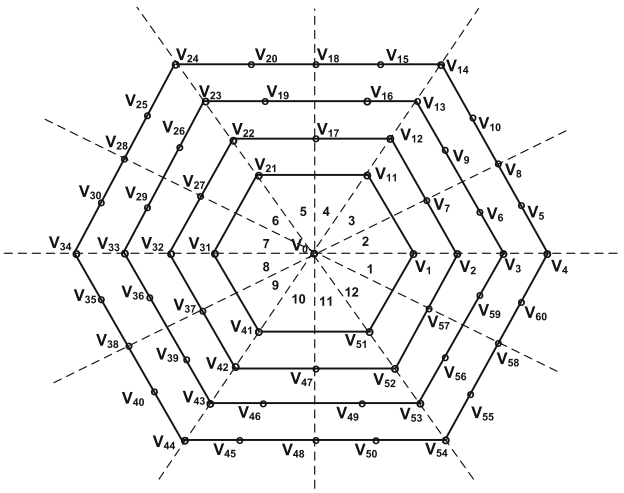

**Fig. 3** Voltage space vector diagram of five-level CHB-MLI

All voltage vectors are distributed in five different magnitude levels and 12 different regions that give the possibility to apply various voltages with different angle and magnitude to the induction motor.

## 4 Five-level CHB-MLI-based conventional DTC

Two hysteresis comparators are used in conventional DTC to minimize the torque and flux errors to zero. The hysteresis comparators are fundamental to DTC scheme because they are responsible for both determining the appropriate voltage vector selection and the period of the voltage vector selected. There are more vector selection possibilities in DTC method by using multilevel inverter.

It has been mentioned that a five-level CHB-MLI has 61 effective switching voltage vectors that can be chosen to minimize the error of torque and flux. To take the most advantage of using a five-level cascaded H-bridge inverter due to the larger number of space vectors, the following strategies are applied:

1. Dividing the stator flux plan into 12 sectors of 30°, starting with the first sector situated between −30 and 0. By increasing the number of sectors to 12, we can obtain a more accurate selection of the inverter switching voltage vectors to minimize the error of the torque and flux to zero, resulting in the improvement of the responses of the flux and torque [25].
2. Applying an 11-level hysteresis comparator to control the torque. Increasing the levels of torque hysteresis controller means defining more levels of error. This causes the controller to differentiate between small and large torque errors. This means that the voltage vectors chosen for the large errors that happen during the start up or doing a step change in torque or flux responses are different from that have been chosen during smaller errors or in the steady state.

Figure 4 shows the torque and flux hysteresis comparator of a five-level CHB-MLI-based conventional DTC. It can be seen that a two-level hysteresis comparator is used to control the flux and an 11-level hysteresis comparator for controlling the torque.

The output of flux hysteresis comparator which is the flux error status has two values, 0 and 1, and the output of the torque hysteresis comparator which is the torque error status has eleven integer values starting from −5 to 5. The optimum selection of the switching voltage vectors for

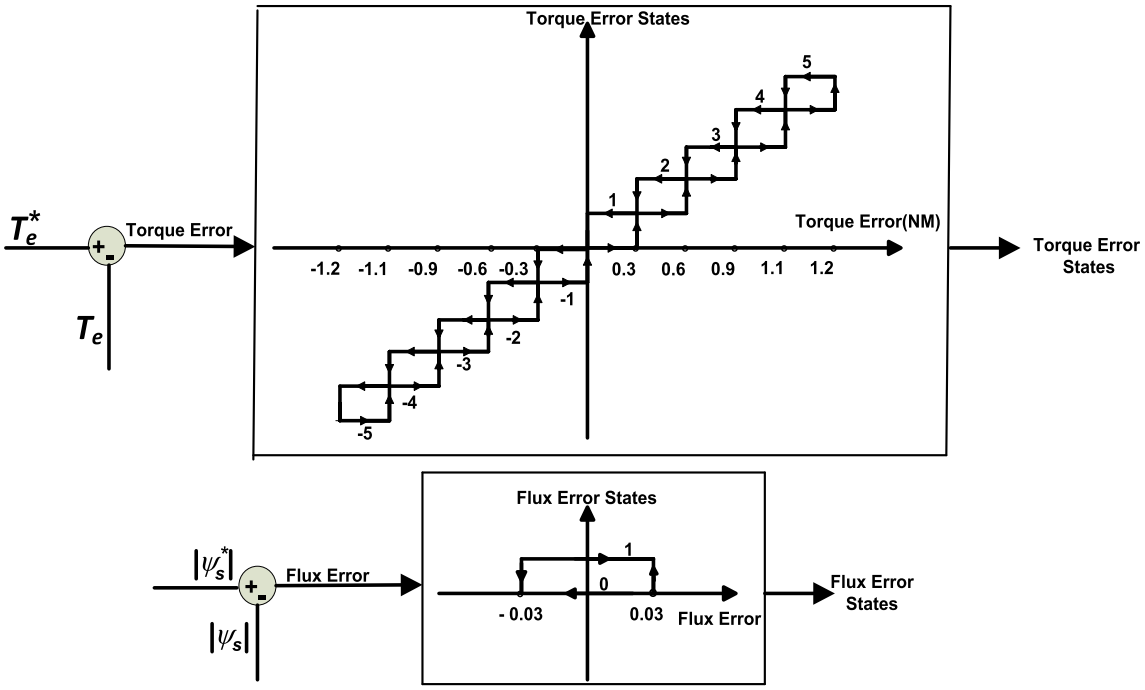


**Fig. 4** Torque and flux hysteresis comparator of five-level CHB-MLI

**Table 1** Voltage vector selection table

| Sector | Torque error state | | | | | | | | | | | |
|---|---|---|---|---|---|---|---|---|---|---|---|---|
| | $S_1$ | $S_2$ | $S_3$ | $S_4$ | $S_5$ | $S_6$ | $S_7$ | $S_8$ | $S_9$ | $S_{10}$ | $S_{11}$ | $S_{12}$ |
| 5 | $v_{14}$ | $v_{18}$ | $v_{24}$ | $v_{28}$ | $v_{34}$ | $v_{38}$ | $v_{44}$ | $v_{48}$ | $v_{54}$ | $v_{58}$ | $v_4$ | $v_8$ |
| 4 | $v_{10}$ | $v_{15}$ | $v_{20}$ | $v_{25}$ | $v_{30}$ | $v_{35}$ | $v_{40}$ | $v_{45}$ | $v_{50}$ | $v_{55}$ | $v_{60}$ | $v_5$ |
| 3 | $v_9$ | $v_{16}$ | $v_{19}$ | $v_{26}$ | $v_{29}$ | $v_{36}$ | $v_{39}$ | $v_{46}$ | $v_{49}$ | $v_{56}$ | $v_{59}$ | $v_6$ |
| 2 | $v_7$ | $v_{12}$ | $v_{17}$ | $v_{22}$ | $v_{27}$ | $v_{32}$ | $v_{37}$ | $v_{42}$ | $v_{47}$ | $v_{52}$ | $v_{57}$ | $v_2$ |
| 1 | $v_{11}$ | $v_{11}$ | $v_{21}$ | $v_{21}$ | $v_{31}$ | $v_{31}$ | $v_{41}$ | $v_{41}$ | $v_{51}$ | $v_{51}$ | $v_1$ | $v_1$ |
| 0 | $v_0$ | $v_0$ | $v_0$ | $v_0$ | $v_0$ | $v_0$ | $v_0$ | $v_0$ | $v_0$ | $v_0$ | $v_0$ | $v_0$ |
| −1 | $v_{51}$ | $v_{51}$ | $v_1$ | $v_1$ | $v_{11}$ | $v_{11}$ | $v_{21}$ | $v_{21}$ | $v_{31}$ | $v_{31}$ | $v_{41}$ | $v_{41}$ |
| −2 | $v_{52}$ | $v_{57}$ | $v_2$ | $v_7$ | $v_{12}$ | $v_{17}$ | $v_{22}$ | $v_{27}$ | $v_{32}$ | $v_{37}$ | $v_{42}$ | $v_{47}$ |
| −3 | $v_{49}$ | $v_{56}$ | $v_{59}$ | $v_6$ | $v_9$ | $v_{16}$ | $v_{19}$ | $v_{26}$ | $v_{29}$ | $v_{36}$ | $v_{39}$ | $v_{46}$ |
| −4 | $v_{50}$ | $v_{55}$ | $v_{60}$ | $v_5$ | $v_{10}$ | $v_{15}$ | $v_{20}$ | $v_{25}$ | $v_{30}$ | $v_{35}$ | $v_{40}$ | $v_{45}$ |
| −5 | $v_{48}$ | $v_{54}$ | $v_{58}$ | $v_4$ | $v_8$ | $v_{14}$ | $v_{18}$ | $v_{24}$ | $v_{28}$ | $v_{34}$ | $v_{38}$ | $v_{44}$ |

clockwise rotation when stator error value is one in all sectors of the stator flux plane can be tabulated by Table 1. The table is used to select the voltage vectors depending on flux error, torque error and the stator flux orientation. When the flux error status is one, the flux increases, and when it is zero the flux decreases (zero state of flux error is not mentioned to reduce complication of table). When the torque error status has the value of 5–1, the torque increases; five has the highest value of increase, and one has the lowest value of increase. When the torque error status is zero, the torque maintains, and when it has the value of −5 to when the torque error status has the value of five to one, the torque increases; five has the highest value of increase, and one has the lowest value of increase. When the torque error status is zero, the torque maintains, and when it has the value of −5 to −1, the torque decreases; −5 has the highest value of decrease, and −1 has the lowest value of decrease.

According to Table 1 and space vector diagram of effective voltages (Fig. 3), a proper voltage has two features; providing suitable torque angle (Eq. 6), which is based on torque error level (Fig. 4) as well as determining the magnitude of stator flux. For example, it is assumed that the stator flux lies in sector 1, and torque error is in the highest level. According to Fig. 3, by applying all voltages in sectors 2 and 3 at the period of $\Delta t$ the angle of torque as well as the magnitude of the stator flux increase, whereas

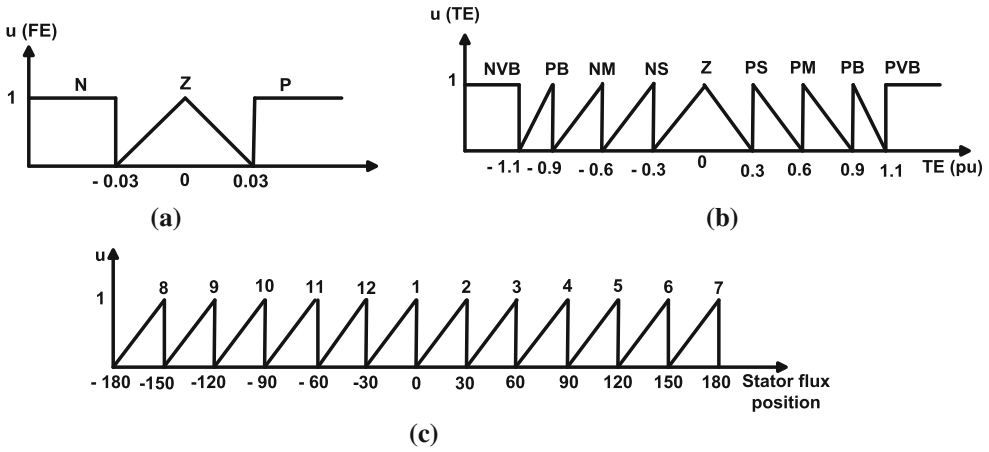


**Fig. 5** Membership functions for the input variables of the fuzzy logic controller. **a** Flux error, **b** torque error, **c** stator flux position

torque error state indicates that a large value of torque should be produced; thus, $v_{14}$ is the proper voltage that has all the mentioned features. Other voltages can be selected according to torque and flux error states.

## 5 Five-level CHB-MLI-based fuzzy DTC

The application of fuzzy logic controller using Mamdani as the inference method to select the output voltage vector has already been investigated in DTC [13]. However, a new fuzzy logic controller using Sugeno as the inference method for selecting the output voltage vector is introduced in this paper, which results in solving the problem of variable switching frequency in conventional DTC by replacing the hysteresis comparators and lookup table. Although Mamdani method is known as the most common fuzzy inference system, Sugeno method is more suitable in some specific applications. Compared with Mamdani method, Sugeno is computationally efficient and provides a more compact representation, which is very useful whenever an adaptive technique is being used for constructing the fuzzy model. By using fuzzy DTC, not only the flux ripples are reduced significantly, but also the total harmonic distortion (THD) of the phase current also decreases since a more sinusoidal current wave is achieved. There are three inputs and one output variables for the fuzzy logic controller. The input variables are the error of the stator flux, the error of the torque and the position of the stator flux. The membership functions for the torque error, stator flux error and stator flux position are as shown in Fig. 5. The linguistic terms used for the error of stator flux and also used for torque membership functions correspond to the stator flux and torque error statuses of Fig. 4 and Table 1. The universe of discourse of the stator flux position has been divided into 12 fuzzy sets ($S_1$–$S_{12}$) corresponding to the sectors in Table 1. The output variable is discrete and includes 61 membership functions having the linguistic terms of $(0, 1, 2, \ldots, 60)$ corresponding to 61 effective inverter switching voltage vectors of the five-level CHB-MLI ($V_0$–$V_{60}$) of Fig. 4. It means that, for example, when the output of the fuzzy logic controller is 10, the inverter switching voltage vector $V_{10}$ is selected to apply to the inverter.

Sugeno's procedure is based on prod-probor decision, and whatever method is used as an inference method for defuzzification. By this method, each value for the stator flux and toque errors and the angle of stator flux is located in a specific membership function. The control output obtained is one of the membership functions of the output variable fed to the inverter. The controller rules have been taken from Table 1. In the description of the membership functions, the correspondence between the linguistic terms and the labels utilized in Table 1 has been explained. The control rules for this controller are presented utilizing the three input and one output variables. The $i$th rule of $R_i$ is written as:

$R_i$: if the flux error is $A_i$, the torque error is $B_i$ and the flux position is $C_i$ then the inverter switching vector is $N_i$

## 6 Simulation results

The effectiveness of the described five-level cascade inverter on torque and flux performance of the induction motor in a same operation condition is verified by using Matlab/Simulink simulation package. DTC drive includes Matlab preset induction motor which has characteristics as: 5.4 Hp (4 kW), 400 V, 50 Hz, two-pole squirrel-cage induction motor with fixed stator resistance ($R_s = 1.435$ ohm). The desired value of electromagnetic torque is 10 Nm, and the desired value of magnitude of stator flux leakage space vector is 0.5 Wb. Conventional two-level DTC and a five-level CHB-MLI besides a five-

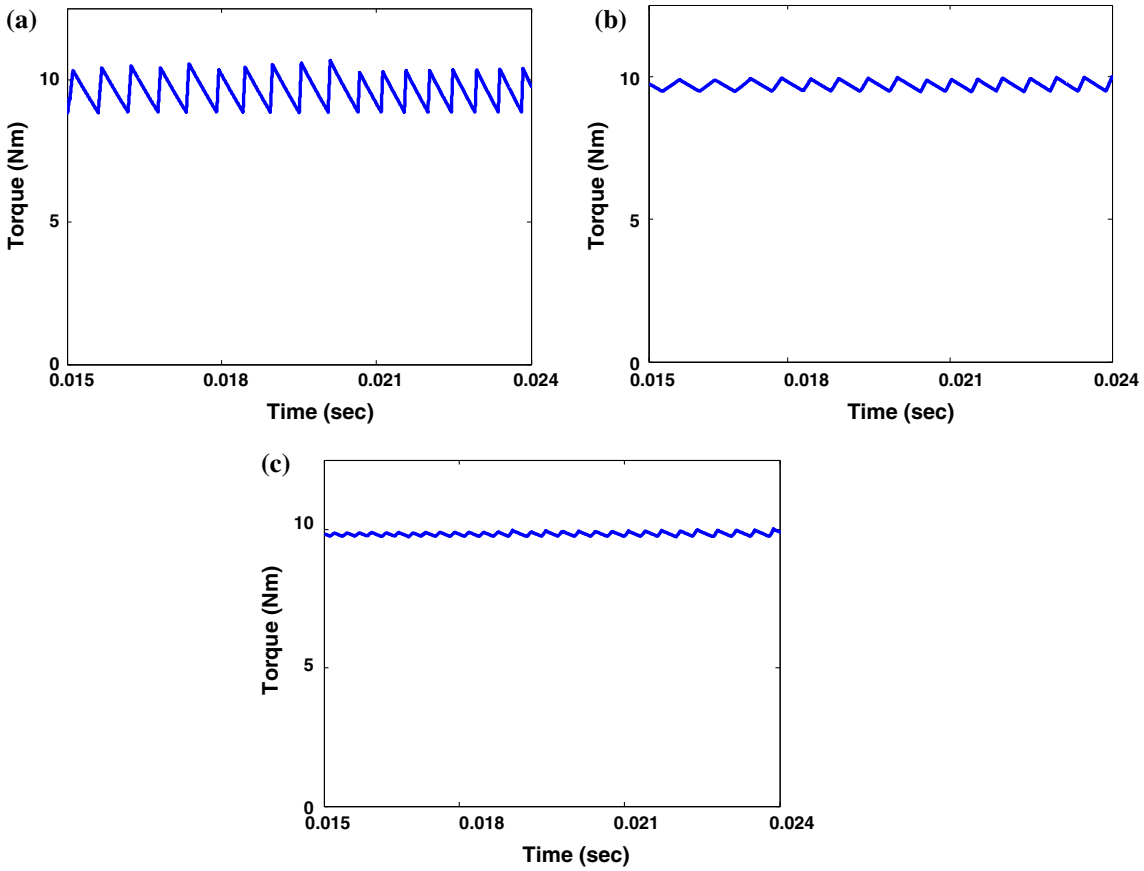


**Fig. 6** **a** Electrical torque of conventional DTC, **b** electrical torque of DTC using five-Level CHB-MLI, **c** electrical torque of DTC using five-Level CHB-MLI with FLC

level CHB-MLI-based fuzzy DTC have been simulated to evaluate and compare their performance.

Figure 6 shows the response of electrical torque in conventional two-level DTC, five-level DTC and five-level DTC-based fuzzy logic controller, respectively. The torque ripple in a conventional DTC is 1 Nm, and it is decreased to <0.5 Nm by using five-level CHB-MLI. The torque ripple is decreased considerably by using fuzzy logic controller instead of hysteresis controller in five-level CHB-MLI. Torque error membership function plays important role in reduction in torque ripple; in fact, fuzzy logic (Fig. 5b) chooses torque error states with more accuracy compared with hysteresis comparator (Fig. 4b). In order to quantitatively compare the results in Fig. 6, the percentage ripple indexed is used as shown in the following equation:

$$\text{percentage ripple} = \frac{\Delta T}{T_{\text{mean}}} \times 100\,\% \tag{10}$$

where $T_{\text{mean}}$ is the average value of the torque waveform, and $\Delta T$ is the variation from the average value. The percentage ripple values are calculated and shown in Table 2. The torque ripple reduction by the proposed method represents better results compared with the two other methods [11, 26].

**Table 2** Percentage ripple values for the torque waveforms obtained by the three methods

| Method used | Fundamental frequency (Hz) | $T_{\text{mean}}$ (Nm) | $\Delta T$ (Nm) | Percentage ripple |
|---|---|---|---|---|
| Conventional DTC | 50 | 9.57 | 1.07 | 11.181 |
| Five-level CHB-MLI in DTC | 50 | 9.71 | 0.39 | 4.016 |
| Five-level CHB-MLI in DTC with FLC | 50 | 9.85 | 0.07 | **0.746** |

Best value obtained is highlighted in bold

Figure 7 shows the stator flux trajectory in three different DTC methods. The stator flux ripple for conventional DTC and (Fig. 7a) five-level CHB-MLI (Fig. 7b) in one cycle is identical because both methods use two-level hysteresis comparator, so there is no change in the flux trajectory scheme. As expected, there is negligible flux ripple (Fig. 7c) by using fuzzy logic controller because it takes the entire values between 0 and 1 as a flux error state, but hysteresis controller output has just two states that cause more flux ripple compared with FLC flux controller.

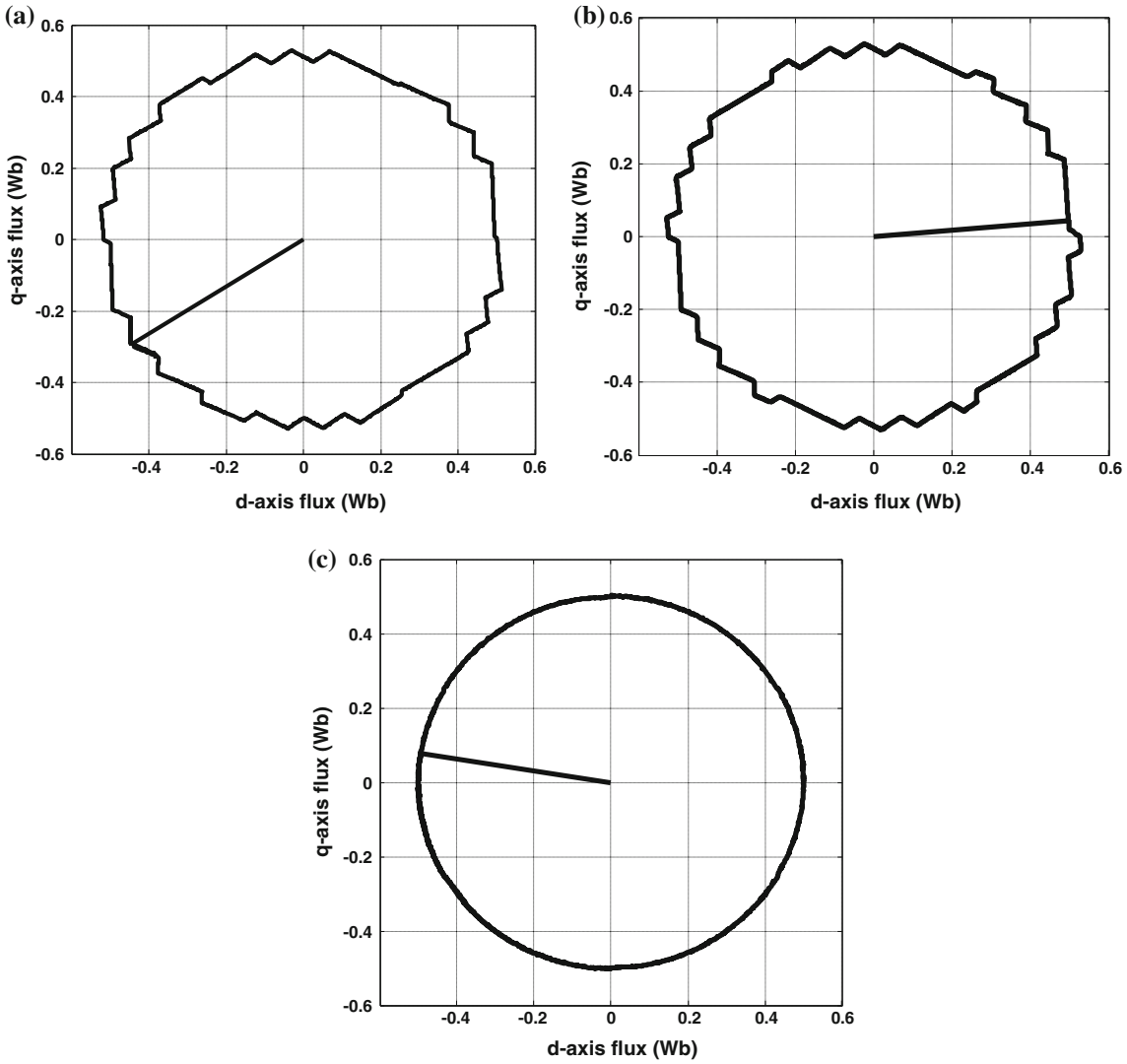


**Fig. 7** Stator flux trajectory. **a** Conventional DTC, **b** five-Level CHB-MLI in DTC, **c** five-level CHB-MLI in DTC with FLC

Figure 8 shows a three-phase stator current in three mentioned methods for DTC. Figure 8a, b indicates that there is no difference in stator current harmonic without FLC application because stator current distortion is generated by stator flux ripple; however, by using FLC stator current (Fig. 8c), distortion decreases much more compared with the two other methods. The THD values for the three waveform demonstrated in Fig. 8 are tabulated in Table 3. Equation (11) is represented for calculating the THD.

$$\mathrm{THD} = \frac{\sqrt{\sum_{i=2}^{n} V_i^2}}{V_1} \tag{11}$$

where $V_1$ represents the amplitude of the fundamental sinusoidal waveform, and $V_i$ is the amplitude of $i$th harmonic. $n$ denotes the maximum harmonic considered, which is equal to 40, in this study.

Moreover, the performance of the proposed method is investigated under transient state of the system. Figure 9 shows the transient response of the proposed controller under variation of the load torque. First, the load torque is changed from 10 to 6, and then again increased to 8. As a result, the amplitude of the stator current is decreased from 8 to 4.3 Amps, at first, and then increased to 5.95 Amps by increment of the load torque. It can be seen that the transient performance of the proposed controller is quite satisfactory, since it can stabilize the stator current after the load torque change, very fast.

## 7 Conclusion

High torque and flux ripples are the two major problems in DTC drives, which draw full attention of most

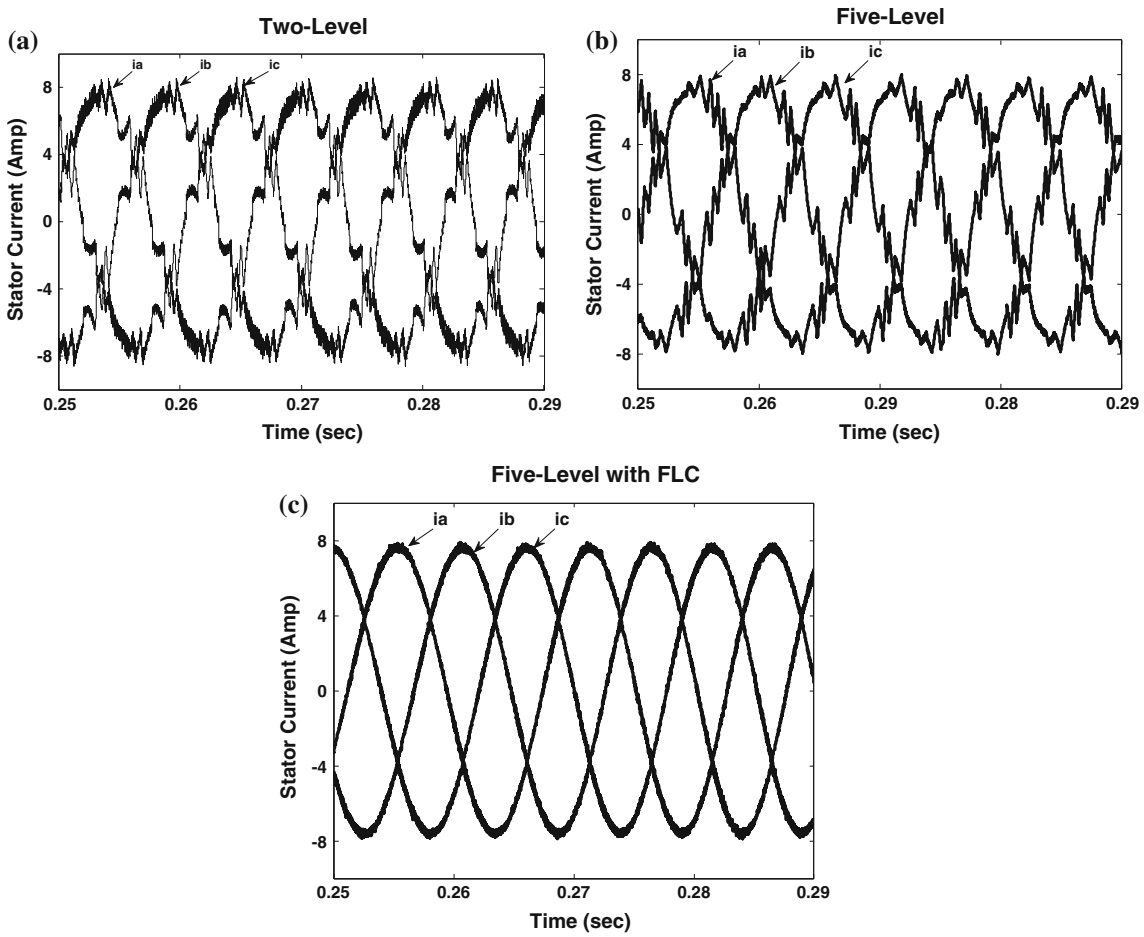


**Fig. 8** Stator three-phase current. **a** Conventional DTC, **b** five-Level CHB-MLI in DTC, **c** five-Level CHB-MLI in DTC with FLC

**Table 3** Total harmonic distortion (THD) values for the stator currents obtained by three methods

| Method used | Fundamental frequency (Hz) | Fifth harmonic percentage | Seventh harmonic percentage | THD |
|---|---|---|---|---|
| Conventional DTC | 50 | 24.91 | 22.82 | 33.76 |
| Five-level CHB-MLI | 50 | 22.58 | 17.61 | 28.34 |
| Proposed DTC with FLC | 50 | **2.85** | **2.54** | **3.82** |

Best values obtained are highlighted in bold

researchers. To overcome these problems, first DTC of induction machines using five-level cascaded H-bridge inverter is proposed that could significantly reduce torque ripples, and then a new fuzzy logic controller using Sugeno as the inference method for selecting the output voltage vector is introduced, which results in more improvement in torque and flux ripple. The simulations results have verified the feasibility of the contributions.

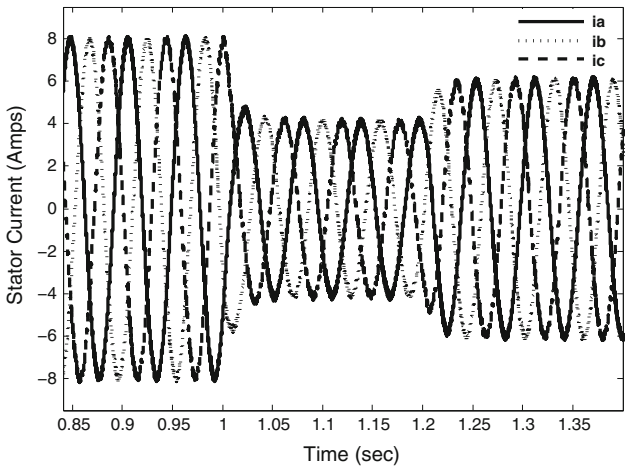


**Fig. 9** Stator three-phase current under load torque change condition

The simulation results have proved that using the five-level cascaded inverter- based DTC is capable of significantly reducing the torque ripples compared with the DTC based on three-level cascade inverter. The simulation results have also verified that using a fuzzy

controller instead of a hysteresis controller has resulted in reduction in the flux ripples significantly as well as reduces the THD of the stator current to below 4 % by making it sinusoidal.

## References


1. Hassan AA, Shehata EG (2012) High performance direct torque control schemes for an IPMSM drive. Electric Power Syst Res 89:171–182
2. Takahashi I, Noguchi T (1986) A new quick-response and high-efficiency control strategy of an induction motor. IEEE Trans Ind Appl IA–22(5):820–827
3. Toufouti R, Meziane S, Benalla H (1997) Direct torque control for induction motor using fuzzy logic. Power Electronics 12.3
4. Abad G, Rodriguez MA, Poza J (2008) Two-level VSC based predictive direct torque control of the doubly fed induction machine with reduced torque and flux ripples at low constant switching frequency. IEEE Trans Power Electron 23(3):1050–1061
5. Casadei D, Serra G, Tani A (1998) Improvement of direct torque control performance by using a discrete svm technique. In: 29th annual IEEE power electronics specialists conference (PESC 98) record, vol 2, pp 997–1003
6. Buja GS, Kazmierkowski MP (2004) Direct torque control of PWM inverter-fed AC motors—a survey. IEEE Trans Ind Electron 51(4):744–757
7. Vas P (1990) Vector control of AC machines. Clarendon Press, Oxford
8. Idris NRN, Yatim AHM (2004) Direct torque control of induction machines with constant switching frequency and reduced torque ripple. IEEE Trans Ind Electron 51(4):758–767
9. Sheng-wei G, Yan C (2010) Torque ripple minimization strategy for direct torque control of induction motors. In: 3rd international conference on intelligent networks and intelligent systems (ICINIS), pp 148–151
10. Casadei D, Serra G, Tani A (1997) Analytical investigation of torque and flux ripple in DTC schemes for induction motors. In: 23rd international conference on industrial electronics, control and instrumentation (IECON 97), vol 2, pp 552–556
11. Habetler TG, Profumo F, Pastorelli M, Tolbert LM (1992) Direct torque control of induction machines using space vector modulation. IEEE Trans Ind Appl 28(5):1045–1053
12. Colak I, Kabalci E, Bayindir R (2011) Review of multilevel voltage source inverter topologies and control schemes. Energy Convers Manag 52(2):1114–1128
13. Mir SA, Zinger DS, Elbuluk ME (1994) Fuzzy controller for inverter fed induction machines. IEEE Trans Ind Appl 30(1):78–84
14. Casadei D, Serra G, Tani A, Zarri L, Profumo F Constant frequency operation of a DTC induction motor drive for electric vehicle. In: Proceedings of the ICEM conference, vol 3, pp 224–229
15. Mir SA, Elbuluk ME, Zinger D (1994) Fuzzy implementation of direct self-control of induction machines. IEEE Trans Ind Appl 30(3):729–735
16. Bird I, Zelaya De La Parra H (1997) Fuzzy logic torque ripple reduction for DTC based AC drives. Electron Iett 33(17):1501–1502
17. Mir S, Elbuluk ME (1995) Precision torque control in inverter-fed induction machines using fuzzy logic. In: 26th annual IEEE power electronics specialists conference (PESC '95) record, vol 1, pp 396–401
18. Rahmani R, Mahmodian MS, Mekhilef S, Shojaei AA (2012) Fuzzy logic controller optimized by particle swarm optimization for DC motor speed control. In: IEEE student conference on research and development (SCOReD), pp 109–113
19. Pati S, Samantray S, Patel NC (2013) A novel adaptive fuzzy controller for performance improvement of direct torque controlled induction generator employed for wind power applications. In: Annual international conference on emerging research areas and international conference on microelectronics, communications and renewable energy (AICERA/ICMiCR), pp 1–6
20. Lekhchine S, Bahi T, Soufi Y (2014) Indirect rotor field oriented control based on fuzzy logic controlled double star induction machine. Int J Electr Power Energy Syst 57:206–211
21. Nayak M, Singh S (2013) Fuzzy logic control of induction motor drive for performance improvement. Doctoral dissertation. National Institute of Technology Rourkela
22. Nabae A, Takahashi I, Akagi H (1981) A new neutral-point-clamped PWM inverter. IEEE Trans Ind Appl 23(5):518–523
23. Rodriguez J, Lai JS, Peng FZ (2002) Multilevel inverters: a survey of topologies, controls, and applications. IEEE Trans Ind Appl 49(4):724–738
24. Casadei D, Profumo F, Serra G, Tani A (2002) FOC and DTC: two viable schemes for induction motors torque control. IEEE Trans Power Electron 17(5):779–787
25. del Toro X, Jayne M, Witting P, Arias A, Romeral J (2004) Direct torque control of an induction motor using a three-level inverter and fuzzy logic. In: IEEE international symposium on industrial electronics, vol 2, pp 923–927
26. Tan Z, Li Y, Li M (2001) A direct torque control of induction motor based on three-level NPC inverter. In: IEEE 32nd annual Power electronics specialists conference (PESC), vol 3, pp 1435–1439
27. Baker RH, Lawrence BH (1975) Electric power converter. US Patent 3,867,643, 18 Feb 1975
28. Vahedi H, Al-Haddad K, Ounejjar Y, Addoweesh K (2013) Crossover switches cell (CSC): a new multilevel inverter topology with maximum voltage levels and minimum DC sources. In: 39th annual conference of the IEEE industrial electronics society (IECON 2013), pp 54–59
29. Vahedi H, Rahmani S, Al-Haddad K (2013) Pinned mid-points multilevel inverter (PMP): three-phase topology with high voltage levels and one bidirectional switch. In: 39th annual conference of the IEEE industrial electronics society (IECON 2013), pp 102–107